

## Supplementary Information

### **Engineering NiFe layered double hydroxide by valence control and intermediates stabilization toward oxygen evolution reaction**

Zhenxing Xu,<sup>#,a</sup> Yiran Ying,<sup>#,b</sup> Guoge Zhang,<sup>\*,a</sup> Kongzhe Li,<sup>a</sup> Yan Liu,<sup>c</sup> Nianqing Fu,<sup>a</sup> Xuyun Guo,<sup>b</sup> Fei Yu,<sup>a</sup> Haitao Huang<sup>\*,b</sup>

<sup>a</sup> School of Materials Science and Engineering, South China University of Technology, No. 381 Wushan Road, Guangzhou, 510641, P. R. China

<sup>b</sup> Department of Applied Physics, The Hong Kong Polytechnic University, No. 11 Yuk Choi Road, Hung Hom, Hong Kong, P. R. China

<sup>c</sup> School of Chemical Engineering and Technology, Sun Yat-sen University, No. 135 Xingang Road West, Guangzhou, 510275, P. R. China

<sup>#</sup> These authors contributed equally to this work.

† Corresponding Authors: ggzhang@scut.edu.cn; aphhuang@polyu.edu.hk.

**Computational Methods:** Density functional theory (DFT) calculations were performed by applying the plane-wave basis and projector-augmented wave (PAW) method,<sup>1</sup> as implemented in the Vienna *ab initio* Simulation Package (VASP).<sup>2</sup> Generalized gradient approximation (GGA) with Perdew–Burke–Ernzerhof (PBE)<sup>3</sup> was used for the exchange-correlation functional. Tkatchenko–Scheffler approach<sup>4</sup> was applied to account for the van der Waals (vdW) interactions. Self-interaction errors for strongly correlated transition metal elements were corrected by using Hubbard U framework with Dudarev rotationally invariant method,<sup>5,6</sup> with U values adopted from the Materials Project database<sup>7</sup> (6.2 eV for Ni, 5.3 eV for Fe). Geometric optimization was allowed until energy convergence criteria of  $10^{-5}$  eV and force convergence criteria  $0.02$  eV Å<sup>-1</sup> were satisfied. Kinetic energy cut-off and Monkhorst–Pack k-point sampling<sup>8</sup> were set as 400 eV and  $5 \times 3 \times 1$  for the single-layer  $2 \times 4 \times 1$  LDH supercell. Atomic ratio was set as Ni:Fe = 7:1 for NiFe LDH and Ni:Fe:Li = 6:1:1 for Li-doped NiFe LDH (NiFe LDH-Li), respectively. A vacuum layer with a thickness of 15 Å was used to minimize the interaction between adjacent image cells. There is still a significant debate on whether Ni or Fe is the active site of an NiFe based OER catalyst.<sup>9,10</sup> Here Ni was selected as the active site since the Ni(III) percentage was directly related with the OER activity.

Gibbs free energy for all intermediates during OER was calculated by adding a quasi-harmonic vibrational free energy correction term  $C_{\text{qh-vib}} = E_{\text{ZPE}} - TS$ , including zero-point energy  $E_{\text{ZPE}}$  and entropy correction – TS to the total energy calculated using density functional theory  $E_{\text{DFT}}$ :

$$G = E_{\text{DFT}} + E_{\text{ZPE}} - TS \quad (1)$$

where  $E_{\text{ZPE}}$  and TS for intermediates in OER are calculated from the vibrational frequencies. In Gibbs free energy calculations, acidic conditions were considered for convenience of calculations (this is thermodynamically equivalent to alkaline conditions)<sup>11,12</sup>. Considering pH=0 and potential against normal hydrogen electrode U=0, Gibbs free energy changes  $\Delta G$  for each intermediate in the four-step OER process were calculated by:

$$\Delta G_{\text{OH}} = G(\text{* OH}) + G(\text{H}^+ + \text{e}^-) - G(\text{*}) - G(\text{H}_2\text{O}) \quad (2)$$

$$\Delta G_{\text{O}} = G(\text{* O}) + 2G(\text{H}^+ + \text{e}^-) - G(\text{*}) - G(\text{H}_2\text{O}) \quad (3)$$

$$\Delta G_{\text{OOH}} = G(\text{* OOH}) + 3G(\text{H}^+ + \text{e}^-) - G(\text{*}) - 2G(\text{H}_2\text{O}) \quad (4)$$

$$\Delta G_1 = \Delta G_{\text{OH}} = G(\text{* OH}) + G(\text{H}^+ + \text{e}^-) - G(\text{*}) - G(\text{H}_2\text{O}) \quad (5)$$

$$\Delta G_2 = \Delta G_{\text{O}} - \Delta G_{\text{OH}} = G(\text{* O}) + G(\text{H}^+ + \text{e}^-) - G(\text{* OH}) \quad (6)$$

$$\Delta G_3 = \Delta G_{\text{OOH}} - \Delta G_{\text{O}} = G(\text{* OOH}) + G(\text{H}^+ + \text{e}^-) - G(\text{* O}) - G(\text{H}_2\text{O}) \quad (7)$$

$$\Delta G_4 = 4.92[\text{eV}] + [G(\text{*}) + G(\text{H}_2\text{O})] - [G(\text{* OOH}) + 3G(\text{H}^+ + \text{e}^-)] \quad (8)$$

Here, Gibbs free energy for one proton and one electron is calculated as

$G(\text{H}^+ + \text{e}^-) = \frac{1}{2}G(\text{H}_2)$  through the conventional hydrogen electrode (CHE) model, and

experimental Gibbs free energy of OER



as  $1.23*4=4.92$  eV<sup>13</sup> were used to calculate  $\Delta G_4$  because of the inaccurate calculation of total energy of  $\text{O}_2$  through DFT.

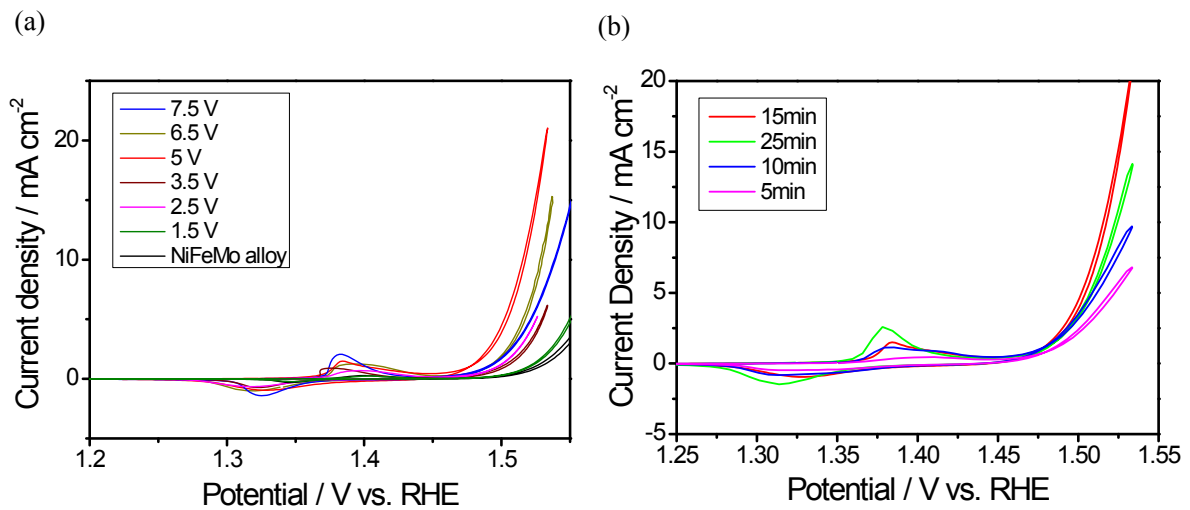


**Figure S1.** Cyclic voltammograms (CVs) of ANF (anodic nickel-based film) obtained at different conditions, a) different voltage for 15 min, and b) 5 V for different time.

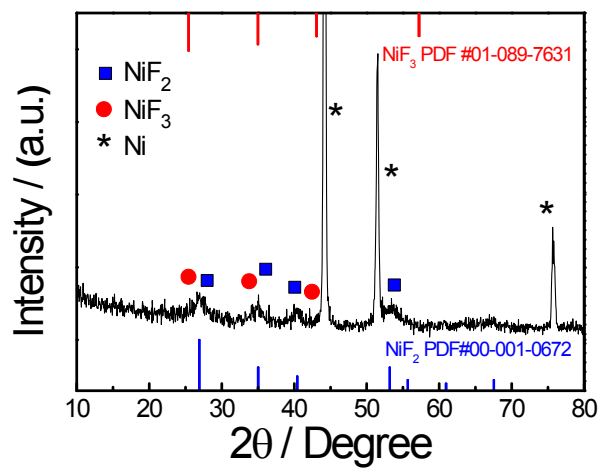


**Figure S2.** XRD pattern of ANF (anodic nickel-based film).

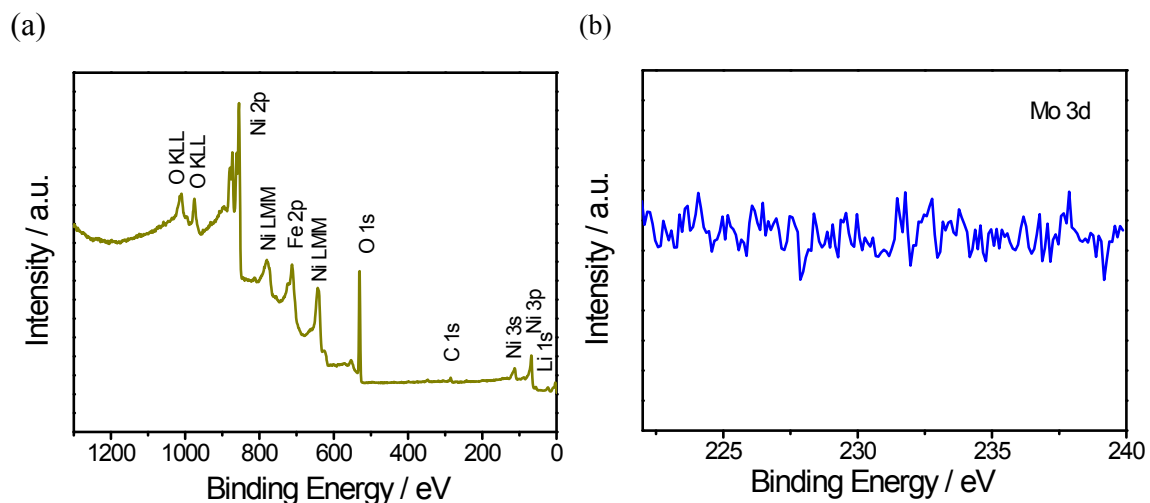


**Figure S3.** XPS of NiFe LDH-Ni(III)Li, a) full spectrum and b) Mo 3d.

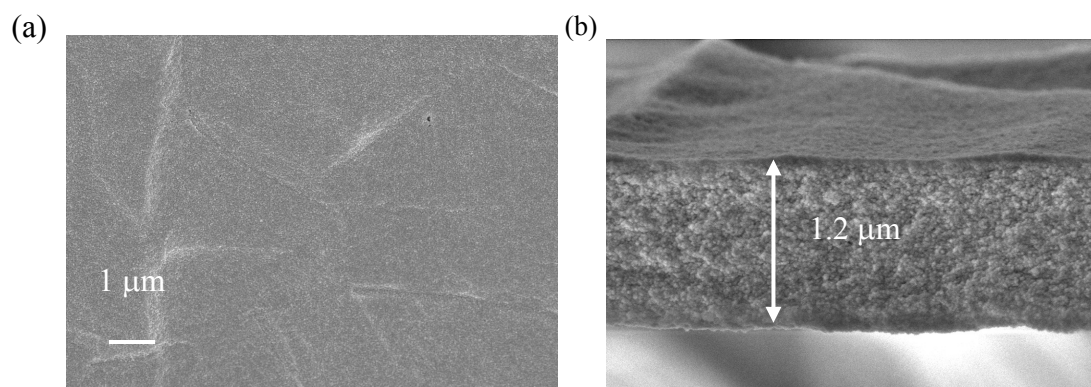


**Figure S4.** SEM images of ANF, a) top view and b) cross-section view.

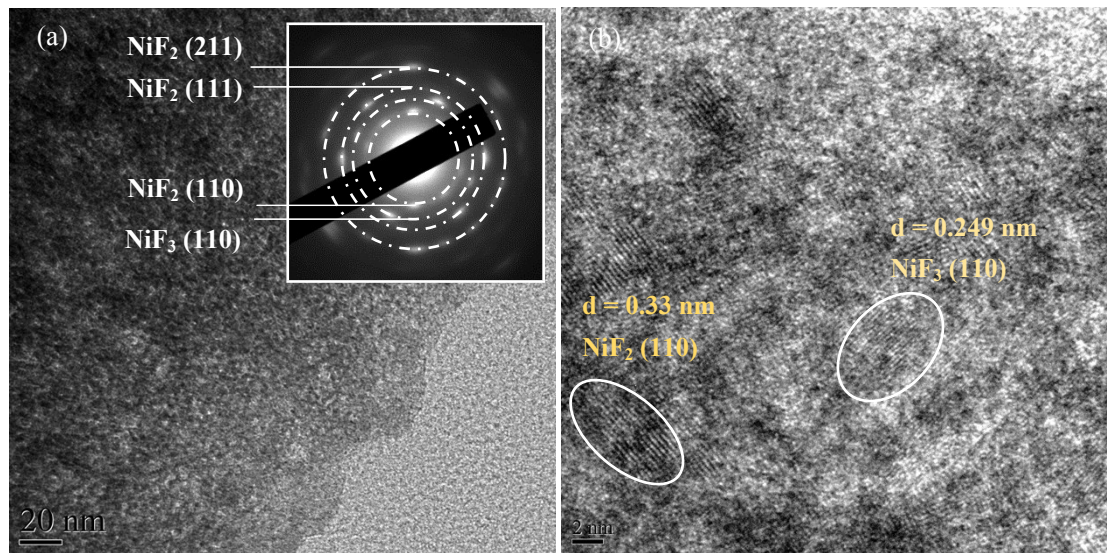


**Figure S5.** TEM images of ANF, a) low magnification and b) high magnification. Inset in a): selected area electron diffraction.

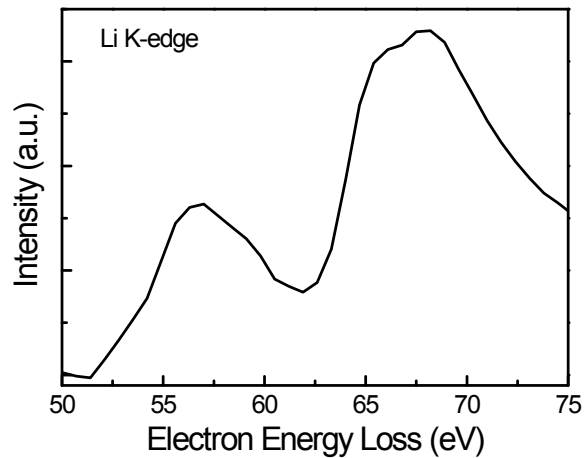


**Figure S6.** Electron energy loss spectroscopy (EELS) spectrum of Li.

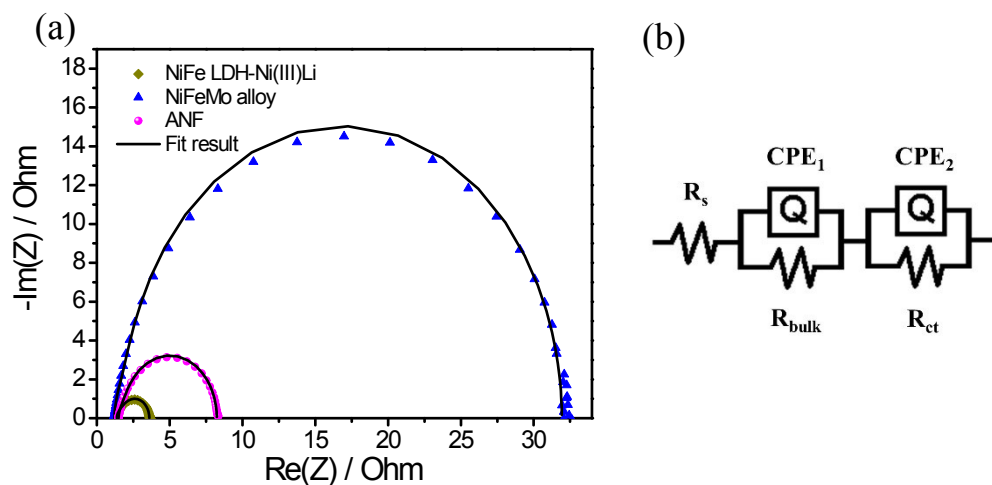


**Figure S7.** a) The Nyquist plot of electrochemical impedance spectroscopy (EIS). b) The equivalent circuit used for the EIS data fitting.

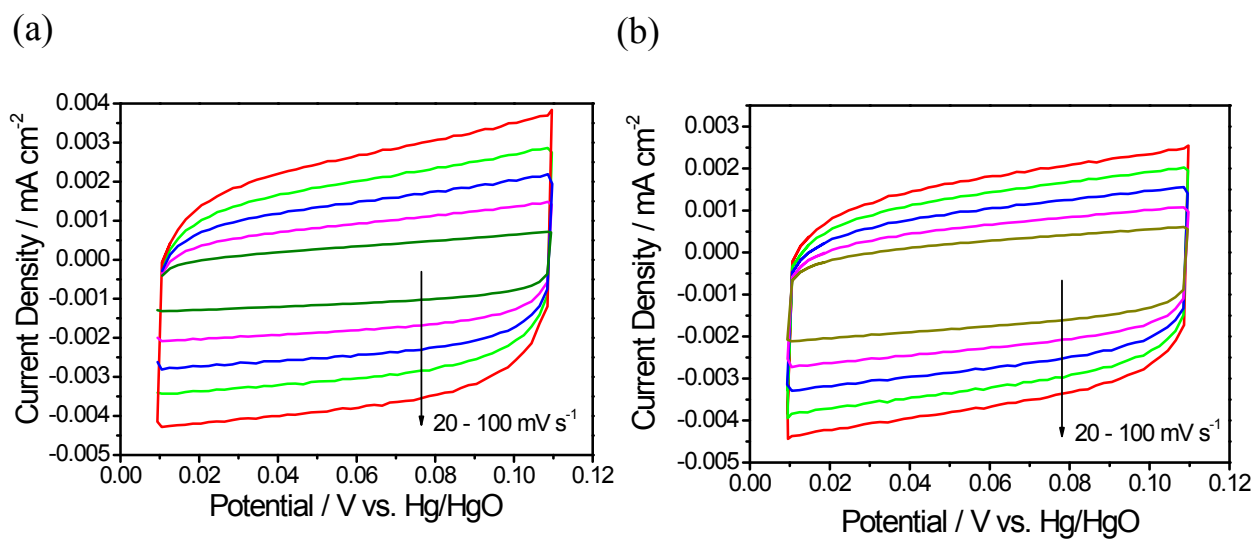


**Figure S8.** CV curves at different scan rates, (a) NiFe LDH-Ni(III)Li and (b) ANF.

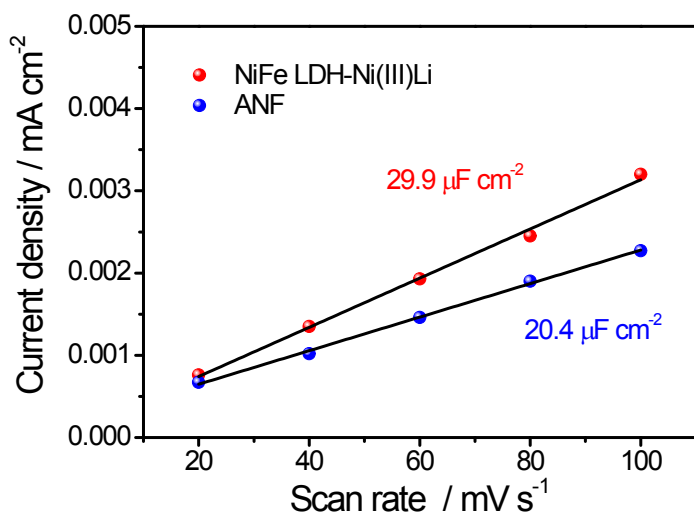


**Figure S9.** The variation of current density with scan rates.

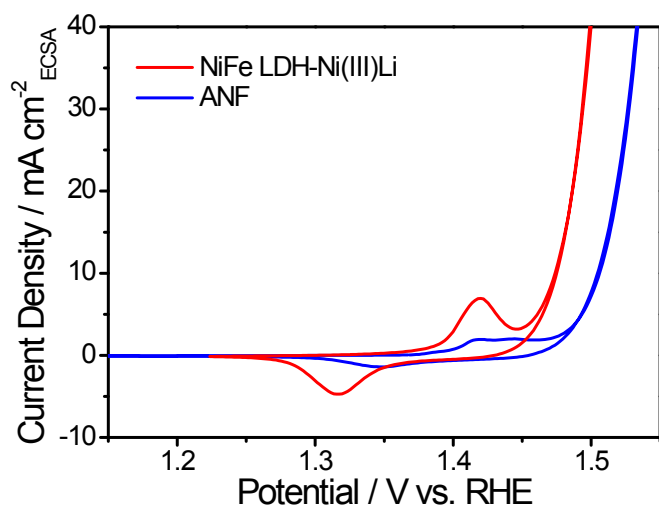


**Figure S10.** Specific activity obtained from the OER current normalized by ECSA.

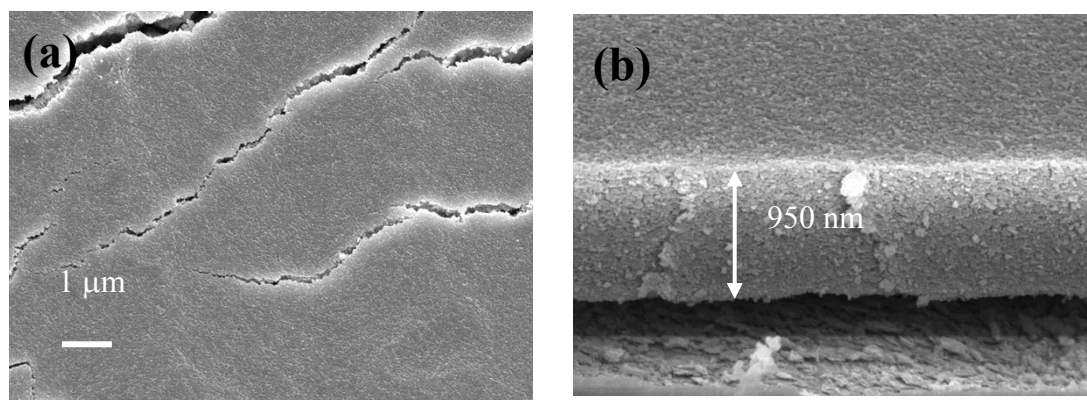


**Figure S11.** SEM images of NiFe LDH-Ni(III)Li after stability test, a) top view and b) cross-section view.

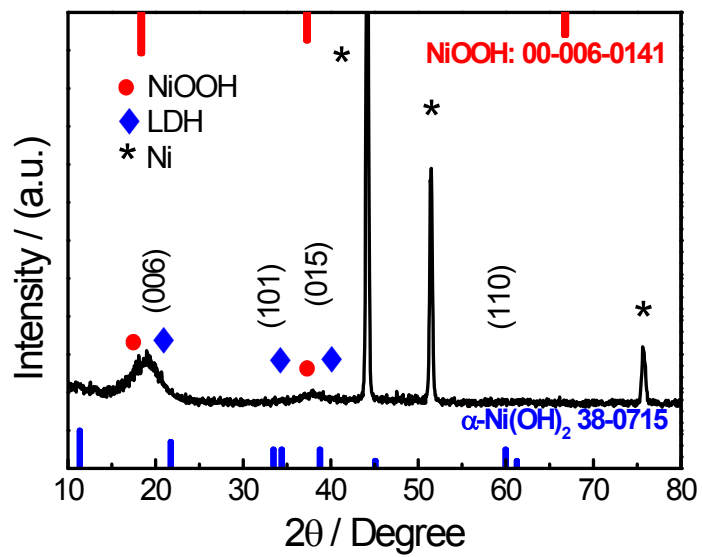


**Figure S12.** XRD of NiFe LDH-Ni(III)Li after stability test.

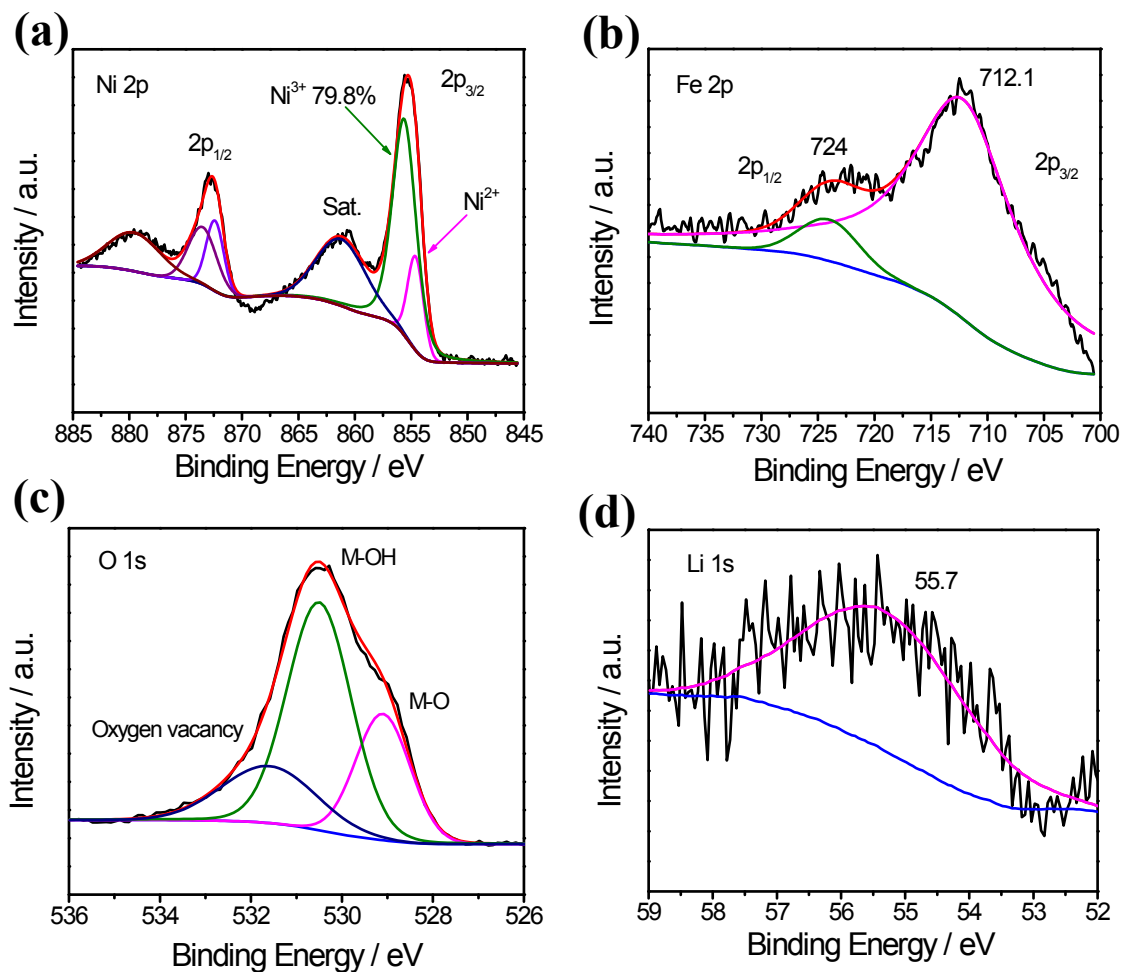


**Figure S13.** XPS of NiFe LDH-Ni(III)Li after stability test, a) Ni 2p, b) Fe 2p, c) O 1s and d) Li 1s.

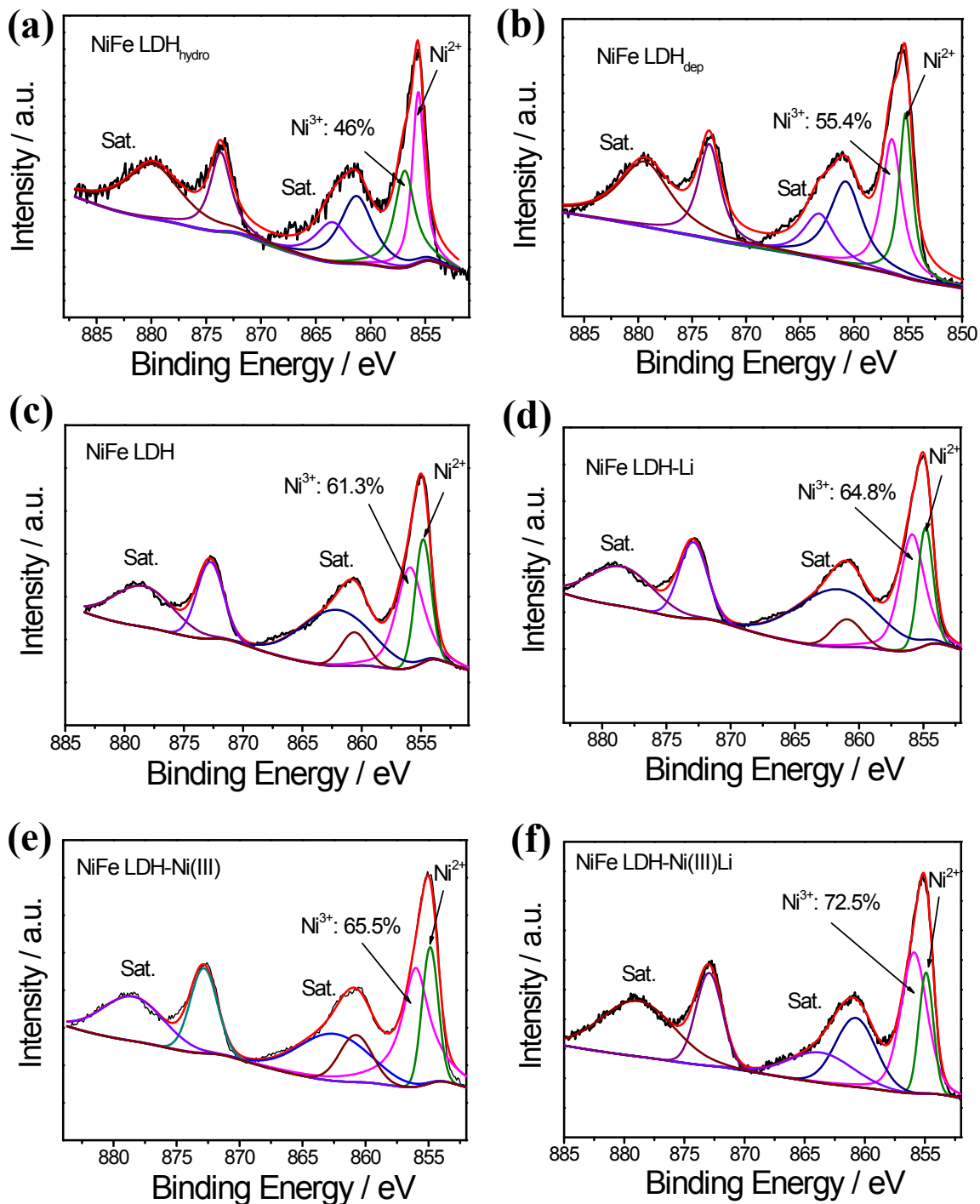


**Figure S14.** Ni 2p XPS of a) NiFe LDH<sub>hydro</sub>, b) NiFe LDH<sub>dep</sub>, c) NiFe LDH, d) NiFe LDH-Li  
e) NiFe LDH-Ni(III) and f) NiFe LDH-Ni(III)Li.

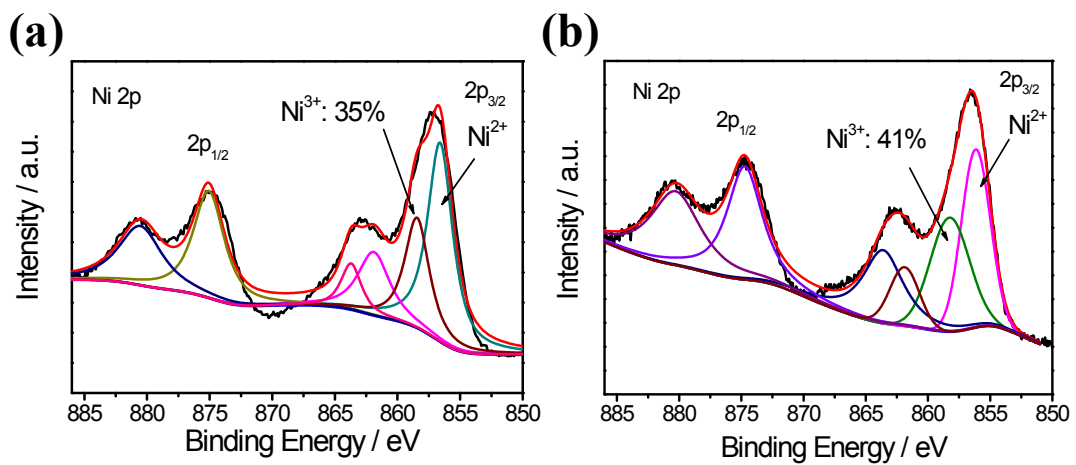


**Figure S15.** Ni 2p XPS of anodic film of a) Ni<sub>4</sub>Fe<sub>1</sub> alloy, b) NiFeMo alloy.

**Table S1.** Synthesis conditions of various NiFe LDH.

Sample Name	Starting material	Anodization	Hydrothermal treatment
NiFe LDH	Ni <sub>4</sub> Fe <sub>1</sub> alloy	5 V for 15 min in the solution with 1 wt.% NH <sub>4</sub> F and 80 wt.% H <sub>3</sub> PO <sub>4</sub>	0.2 M NaOH, 120°C 4h
NiFe LDH-Li	Ni <sub>4</sub> Fe <sub>1</sub> alloy	the solution with 1 wt.% NH <sub>4</sub> F and 80 wt.% H <sub>3</sub> PO <sub>4</sub>	0.2 M LiOH, 120°C 4h
NiFe LDH-Ni(III)	NiFeMo alloy		0.2 M NaOH, 120°C 4h
NiFe LDH-Ni(III)Li	NiFeMo alloy		0.2 M LiOH, 120°C 4h

**Table S2.** Chemical composition of ANF.

Elements	wt. %	at. %
O	5.9	13.8
F	20.7	40.6
Fe	8.5	5.7
Ni	59.8	37.9
Mo	5.0	1.9

**Table S3.** Comparison of OER activity

<b>Electrocatalyst</b>	<b>Current collector</b>	<b>Electrolyte</b>	<b><math>\eta_{10}</math> (mV)</b>	<b>Tafel Slope (mV dec<sup>-1</sup>)</b>	<b>Reference</b>
NiFe LDH-Ni(III)Li	Flat, NiFeMo alloy foil	1M KOH	248	35	This work
Co-NC/CF <sup>14</sup>	Carbon fiber cloth	1M KOH	246	72	Energy Environ. Sci., 2020
FeCo/Co <sub>2</sub> P@NPCF <sup>15</sup>	Carbon nanofiber	0.1 M KOH	330	61	Adv. Energy Mater. 2020
CoFeZr oxides/NF <sup>16</sup>	3D, nickel foam	1M KOH	$\eta_{20} = 264$ mV	54.2	Adv. Mater. 2019
V doped CoFe-LDH <sup>17</sup>	Carbon papers	1 M KOH	242	41.4	Nanoscale, 2019
Ultrathin Ni-Fe LDH <sup>18</sup>	3D, nickel foam	1 M KOH	210	31	ACS Catal. 2019
NiCoFe/NiCoFeO NTAs <sup>19</sup>	Carbon fiber cloth	1M NaOH	201	39	J. Am. Chem. Soc., 2019
Co-N <sub>x</sub> /C nanorod <sup>20</sup>	Glassy carbon	0.1 M KOH	300	62.3	Adv. Funct. Mater. 2018
NiFeCr-LDH <sup>21</sup>	Carbon fiber cloth	1 M KOH	280	52	Adv. Energy Mater., 2018
Single-unit-cell-thick CoFe-LDH <sup>22</sup>	Glassy carbon	0.1 M KOH	280	33.4	Nano Res., 2018
CoFe-LDH with rich defects <sup>23</sup>	Glassy carbon	1 M KOH	302	41	Chem. Commun., 2018
NiFeMn LDHs <sup>24</sup>	Glassy carbon	1 M KOH	289	47	Chem. Commun.,

2016

Na <sub>0.08</sub> Ni <sub>0.9</sub> Fe <sub>0.1</sub> O <sub>2</sub> <sup>25</sup>	Glassy carbon	1 M KOH	260	40	Energy Environ. Sci., 2017
FeNi-LDH /Ti <sub>3</sub> C <sub>2</sub> -MXene <sup>26</sup>	Glassy carbon	1 M KOH	298	43	Nano Energy, 2018
CoOx <sup>27</sup>	Glassy carbon	1 M KOH	306	65	Nano Energy, 2018
CoO <sub>x</sub> /BNG <sup>28</sup>	Glassy carbon	0.1 M KOH	295	57	Angew. Chem. Int. Ed., 2017
pc-Ni-Bi@NB <sup>29</sup>	Glassy carbon	1 M KOH	302	52	Angew. Chem. Int. Ed., 2017
Ni <sub>x</sub> Co <sub>1-x</sub> O <sup>30</sup>	Planar, gold	0.5 M KOH	350		Adv. Funct. Mater. 2017
Fe <sub>3</sub> N/Fe <sub>4</sub> N <sup>31</sup>	3D, nickel foam	1M KOH	238	44.5	ACS Catal. 2017
NiO/CoN <sup>32</sup>	Carbon fiber paper	1M KOH	300	35	ACS Nano, 2017
Fe <sub>1</sub> Co <sub>1</sub> -ONS <sup>33</sup>	Glassy carbon	0.1M KOH	308	36.8	Adv. Mater. 2017
NiFe-MOF <sup>34</sup>	3D, nickel foam	0.1M KOH	240	34	Nat. Commun., 2017
NiFe/NiFe:Pi <sup>35</sup>	Carbon fiber paper	1M KOH	290	38	ACS Catal. 2017
CoFe LDH-Ar <sup>36</sup>	Glassy carbon	1M KOH	266	37.85	Angew. Chem. Int. Ed., 2017

**Table S4.** Fitting result of the equivalent circuit.

	$R_s / \Omega$	$CPE_1 / mF$	$R_{bulk} / \Omega$	$CPE_2 / mF$	$R_{ct} / \Omega$
NiFe LDH-Ni(III)Li	1.372	37.3	0.334	42.2	3.294
ANF	1.513	39.7	0.428	48.7	6.397
NiFeMo alloy	1.215	1.427	0.974	2.2	30

**Table S5.** Elements concentration in the test solution (1M KOH) as detected by ICP-MS (Inductively Coupled Plasma Mass Spectrometry).

Electrolyte (1M KOH)	Elements (mg/L)	Ni	Fe	Mo	Li
Before test	<0.01	0.0116	<0.01	0.0131	
After stability test	<0.01	0.0158	<0.01	0.0141	

**Table S6.** DFT-calculated total energy  $E_{DFT}$ , zero-point energy  $E_{ZPE}$ , and entropic contribution term TS for all intermediates (on NiFe LDH and NiFe LDH-Li) and gases in OER. Values of TS for gases are extracted from experimental data in CRC Handbook<sup>13</sup>. \* denotes active sites in the OER (Ni atoms in this work).

System	$E_{DFT}$ (eV)	$E_{ZPE}$ (eV)	TS (eV)
<b>H<sub>2</sub></b>	-6.737	0.269	0.403
<b>H<sub>2</sub>O</b>	-14.151	0.567	0.670
*	-185.809	0	0
<b>NiFe LDH</b>	<b>*O</b>	-189.012	0.036
	<b>*OH</b>	-195.724	0.306
			0.028

	<b>*OOH</b>	-199.976	0.425	0.124
	*	-142.649	0	0
<b>NiFe LDH-</b>	<b>*O</b>	-146.025	0.029	0.112
<b>Li</b>	<b>*OH</b>	-152.515	0.282	0.093
	<b>*OOH</b>	-156.887	0.410	0.171

**Table S7.** DFT-calculated adsorption energy  $\Delta E$  and adsorption free energy  $\Delta G$  (in eV) for all intermediates in OER.

<b>System</b>	<b>NiFe LDH</b>	<b>NiFe LDH-Li</b>
$\Delta E_{OH}$	0.90	1.52
$\Delta E_O$	4.18	4.41
$\Delta E_{OOH}$	4.03	4.23
$\Delta G_{OH}$	1.18	1.71
$\Delta G_O$	4.16	4.40
$\Delta G_{OOH}$	4.34	4.50

## References

1. P. E. Blöchl, *Phys. Rev. B*, 1994, **50**, 17953-17979.
2. G. Kresse and J. Furthmüller, *Phys. Rev. B*, 1996, **54**, 11169-11186.
3. J. P. Perdew, K. Burke and M. Ernzerhof, *Phys. Rev. Lett.*, 1996, **77**, 3865-3868.
4. A. Tkatchenko and M. Scheffler, *Phys. Rev. Lett.*, 2009, **102**, 073005.
5. V. I. Anisimov, J. Zaanen and O. K. Andersen, *Phys. Rev. B*, 1991, **44**, 943-954.
6. S. Dudarev, G. Botton, S. Savrasov, C. Humphreys and A. Sutton, *Phys. Rev. B*, 1998, **57**, 1505.
7. A. Jain, S. P. Ong, G. Hautier, W. Chen, W. D. Richards, S. Dacek, S. Cholia, D. Gunter, D. Skinner, G. Ceder and K. A. Persson, *APL Mater.*, 2013, **1**, 011002.
8. H. J. Monkhorst and J. D. Pack, *Phys. Rev. B*, 1976, **13**, 5188-5192.
9. F. Song, L. Bai, A. Moysiadou, S. Lee, C. Hu, L. Liardet and X. Hu, *J. Am. Chem. Soc.*, 2018, **140**, 7748-7759.
10. J. Song, C. Wei, Z.-F. Huang, C. Liu, L. Zeng, X. Wang and Z. J. Xu, *Chem. Soc. Rev.*, 2020, **49**, 2196-2214.
11. M. Bajdich, M. García-Mota, A. Vojvodic, J. K. Nørskov and A. T. Bell, *J. Am. Chem. Soc.*, 2013, **135**, 13521-13530.
12. M. García-Mota, M. Bajdich, V. Viswanathan, A. Vojvodic, A. T. Bell and J. K. Nørskov, *J Phys. Chem. C*, 2012, **116**, 21077-21082.
13. *CRC Handbook of Chemistry and Physics*, CRC Press, Boca Raton, FL, 93rd edn., 2012.
14. H. Huang, S. Zhou, C. Yu, H. Huang, J. Zhao, L. Dai and J. Qiu, *Energy Environ. Sci.*, 2020, **13**, 545-553.
15. Q. Shi, Q. Liu, Y. Ma, Z. Fang, Z. Liang, G. Shao, B. Tang, W. Yang, L. Qin and X. Fang, *Adv. Energy Mater.*, 2020, **10**, 1903854.
16. L. Huang, D. Chen, G. Luo, Y.-R. Lu, C. Chen, Y. Zou, C.-L. Dong, Y. Li and S. Wang, *Adv. Mater.*, 2019, **31**, 1901439.
17. Y. Yang, Y. Ou, Y. Yang, X. Wei, D. Gao, L. Yang, Y. Xiong, H. Dong, P. Xiao and Y. Zhang, *Nanoscale*, 2019, **11**, 23296-23303.
18. C. Kuai, Y. Zhang, D. Wu, D. Sokaras, L. Mu, S. Spence, D. Nordlund, F. Lin and X.-W. Du, *ACS Catal.*, 2019, **9**, 6027-6032.
19. Y. Liu, Y. Ying, L. Fei, Y. Liu, Q. Hu, G. Zhang, S. Y. Pang, W. Lu, C. L. Mak, X. Luo, L. Zhou, M. Wei and H. Huang, *J. Am. Chem. Soc.*, 2019, **141**, 8136-8145.
20. I. S. Amiinu, X. Liu, Z. Pu, W. Li, Q. Li, J. Zhang, H. Tang, H. Zhang and S. Mu, *Adv. Funct. Mater.*, 2018, **28**, 1704638.
21. Y. Yang, L. Dang, M. J. Shearer, H. Sheng, W. Li, J. Chen, P. Xiao, Y. Zhang, R. J. Hamers and S. Jin, *Adv. Energy Mater.*, 2018, **8**, 1703189.
22. R. Gao and D. Yan, *Nano Res.*, 2018, **11**, 1883-1894.
23. P. Zhou, Y. Wang, C. Xie, C. Chen, H. Liu, R. Chen, J. Huo and S. Wang, *Chem. Commun.*, 2017, **53**, 11778-11781.
24. Z. Lu, L. Qian, Y. Tian, Y. Li, X. Sun and X. Duan, *Chem. Commun.*, 2016, **52**, 908-911.
25. B. Weng, F. Xu, C. Wang, W. Meng, C. R. Grice and Y. Yan, *Energy Environ. Sci.*, 2017, **10**, 121-128.
26. M. Yu, S. Zhou, Z. Wang, J. Zhao and J. Qiu, *Nano Energy*, 2018, **44**, 181-190.
27. W. Xu, F. Lyu, Y. Bai, A. Gao, J. Feng, Z. Cai and Y. Yin, *Nano Energy*, 2018, **43**, 110-116.
28. Y. Tong, P. Chen, T. Zhou, K. Xu, W. Chu, C. Wu and Y. Xie, *Angew. Chem. Int. Edit.*, 2017, **56**, 7121-7125.

29. W.-J. Jiang, S. Niu, T. Tang, Q.-H. Zhang, X.-Z. Liu, Y. Zhang, Y.-Y. Chen, J.-H. Li, L. Gu, L.-J. Wan and J.-S. Hu, *Angew. Chem. Int. Edit.*, 2017, **56**, 6572-6577.
30. K. Fominykh, G. C. Tok, P. Zeller, H. Hajiyani, T. Miller, M. Döblinger, R. Pentcheva, T. Bein and D. Fattakhova-Rohlfing, *Adv. Funct. Mater.*, 2017, **27**, 1605121-n/a.
31. F. Yu, H. Zhou, Z. Zhu, J. Sun, R. He, J. Bao, S. Chen and Z. Ren, *ACS Catal.*, 2017, **7**, 2052-2057.
32. J. Yin, Y. Li, F. Lv, Q. Fan, Y.-Q. Zhao, Q. Zhang, W. Wang, F. Cheng, P. Xi and S. Guo, *ACS Nano*, 2017, **11**, 2275-2283.
33. L. Zhuang, L. Ge, Y. Yang, M. Li, Y. Jia, X. Yao and Z. Zhu, *Adv. Mater.*, 2017, **29**, 1606793-n/a.
34. J. Duan, S. Chen and C. Zhao, *Nat. Commun.*, 2017, **8**, 15341.
35. Y. Li and C. Zhao, *ACS Catal.*, 2017, **7**, 2535-2541.
36. Y. Wang, Y. Zhang, Z. Liu, C. Xie, S. Feng, D. Liu, M. Shao and S. Wang, *Angew. Chem. Int. Edit.*, 2017, **56**, 5867-5871.